

Fractionated crystallization in a polydisperse mixture of hard spheres

Paul Bartlett

Department of Chemistry, University of Bath, Bath, BA2 7AY, United Kingdom

(Received 10 July 1998; accepted 18 September 1998)

We consider the nature of the fluid–solid phase transition in a polydisperse mixture of hard spheres. For a sufficiently polydisperse mixture ($\sigma > 0.085$) crystallization occurs with simultaneous fractionation. At the fluid–solid boundary, a broad fluid diameter distribution is split into a number of narrower fractions, each of which then crystallize. The number of crystalline phases increases with the overall level of polydispersity. At high densities, freezing is followed by a sequence of demixing transitions in the polydisperse crystal. © 1998 American Institute of Physics. [S0021-9606(98)51548-6]

I. INTRODUCTION

Equal-sized hard spheres constitute probably the simplest example of a purely entropic material. In a hard-sphere system there is no contribution to the internal energy U from interparticle forces so that U is a constant, at a fixed temperature. Minimizing the free energy, $F = U - TS$, is thus simply equivalent to maximizing the entropy S . Consequently, the structure and phase behavior of hard spheres is determined solely by entropy. Although the hard-sphere model was originally introduced as a mathematically simple model of atomic liquids¹ recent work has demonstrated its usefulness as a basic model for complex fluids.² Suspensions of submicron poly(methyl methacrylate) or silica colloids, coated with a thin polymeric layer so that strong repulsions dominate the attractive dispersion forces between the colloidal cores, behave in many ways as hard spheres. In the last decade, a great deal of effort has been devoted to systematic studies of such colloidal ‘hard-sphere’ systems.³ For sufficiently monodisperse colloids, crystallization is observed at densities similar to those predicted by computer simulation for hard spheres.^{4,5} Measurements of the osmotic pressure and compressibility show a similar dramatic agreement with predicted hard-sphere properties.³

There is, however, one important and unavoidable difference between colloids and the classical hard-sphere model which is frequently overlooked. Whereas the spheres in the classical model are identically sized (i.e., monodisperse) colloidal particles have an inevitable spread of sizes which is most conveniently characterized by the polydispersity, σ , defined as

$$\sigma = (\overline{R^2} - \bar{R}^2)^{1/2} / \bar{R}, \quad (1)$$

where

$$\overline{\rho R^n} = \int dR \rho(R) R^n, \quad (2)$$

with $\rho(R)$ the density distribution and $\rho = \int dR \rho(R)$.

Recent work has revealed that as soon as a hard-sphere suspension is allowed to enjoy a significant degree of polydispersity, several interesting new phenomena arise. Experiments find that the crystallization transition is suppressed

altogether at $\sigma \approx 0.12$ while samples with $\sigma = 0.075$ crystallize only slowly in the coexistence region and not above the melting transition.³ Other examples of the effects of polydispersity are the appearance of a demixing transition in a polydisperse fluid of hard spheres^{6,7} and the observation of a liquid–vapor transition in polydisperse adhesive hard spheres.⁸

The effect of polydispersity on the crystallization of hard-sphere colloids has been investigated by computer simulation,^{9–11} density functional,^{12,13} and analytical theories.^{14,15} The picture that emerges is remarkably consistent. All calculations find that the fluid–solid phase transition vanishes for polydispersities above a certain critical level σ_c . The phase diagram for small polydispersities ($\sigma \leq \sigma_c$) has been rationalized¹⁵ in terms of the appearance of an additional high density crystal-to-fluid transition, in a polydisperse system. While, at low polydispersities hard spheres display, with increasing density, the conventional fluid-to-crystal transition, at higher polydispersities re-entrant behavior is predicted. The two freezing transitions converge to a single point in the (ϕ, σ) plane which is a polydisperse analogue of the point of equal concentration found in molecular mixtures.¹⁶ At this singularity, the free energies of the polydisperse fluid and crystal phases are equal.

The purpose of this note is to examine the fate of a highly polydisperse ($\sigma > \sigma_c$) hard-sphere fluid. Previous theoretical research has not been able to identify a fluid–solid transition for $\sigma > \sigma_c$ so it is generally believed that the equilibrium phase is disordered at all densities up to close packing. Several years ago, Pusey¹⁷ suggested that a highly polydisperse suspension might crystallize by splitting the broad overall distribution into a number of narrower distributions of polydispersity σ_s , each of which could be accommodated within a single crystalline phase. Each crystal would then have a correspondingly different mean size with the number of crystalline phases increasing with the overall polydispersity. For fractionated crystallization to occur the total free energy of the set of multiple crystals must be lower than that of the equivalent polydisperse fluid. This can only happen if the reduction in free energy as particles are removed from a fluid and placed in a crystal is sufficiently large to exceed the loss of entropy of mixing as the distribution is partitioned.

This is a delicate balance and it is far from obvious where the result lies. Pusey, for instance, originally suggested that fractionation would generate crystals with a polydispersity of σ_c so as to minimize the number of crystal phases required and the subsequent loss of entropy of mixing. However, as noted above, at σ_c the free energy of the polydisperse fluid and crystal phases are equal¹⁵ and so there is no driving force for fractionation.

In earlier work¹⁵ the possibility of fractionated crystallization for $\sigma > \sigma_c$ was considered but no conditions where two crystal phases could coexist could be found. Here we re-examine the stability of a polydisperse hard-sphere fluid using a much simpler approach. Rather than solving the equations of phase equilibria in a polydisperse system we restrict ourselves to the easier task of comparing the free energies, at the same density and temperature, of crystal and fluid phases. We find, in agreement with Pusey,¹⁷ that fractionation occurs in polydisperse hard-sphere mixtures but that the polydispersity of the resulting crystals is substantially less than σ_c .

The rest of the paper is organized as follows: in Sec. II we present our model for the free energies of the polydisperse fluid and crystal phases. The stability diagram is presented in Sec. III. Finally, in Sec. IV we summarize and conclude.

II. THE MODEL

Our model consists of N hard-sphere particles in a volume V , at an overall density of $\rho = N/V$. Each particle has a diameter R drawn from some overall distribution $\rho(R)$ so that $\rho = \int dR \rho(R)$. Previous work has suggested¹⁷ that the thermodynamic properties of a polydisperse system are relatively insensitive to the detailed *shape* assumed for the diameter distribution, at least when the polydispersity is small ($\sigma < 0.1$). Indeed the phase behavior has been found,¹⁸ to a rather good approximation, to be a function only of the first three moments of the diameter distribution, ρ , \bar{R} , and the normalized width σ . For a broad diameter distribution, higher moments will presumably also need to be considered. Consequently, the phase behavior will become increasingly sensitive to the shape of the distribution assumed. However, we expect that the width of the distribution will still play an important if not the dominant role in determining the generic features of the phase behavior of a polydisperse system. Since our concern here is with establishing these general features of the polydisperse phase diagram we have taken $\rho(R)$ as a simple rectangular distribution,

$$\rho(R) = \rho \begin{cases} 0 & R < \bar{R}(1 - w/2) \\ (\bar{R}w)^{-1} & \bar{R}(1 - w/2) \leq R \leq \bar{R}(1 + w/2), \\ 0 & R > \bar{R}(1 + w/2) \end{cases} \quad (3)$$

where \bar{R} is the mean diameter and the normalized width w is related directly to the conventional polydispersity σ by $w = 2\sqrt{3}\sigma$. It will prove convenient to choose as variables the mean diameter \bar{R} , the polydispersity σ and the volume fraction $\phi = (\pi/6) \int dR \rho(R) R^3 = (\pi/6) \rho \bar{R}^3 (1 + w^2/4)$.

Our first task is to calculate the thermodynamics of the fluid state. The free energy density ($f = F/V$) may be conveniently split into ideal and excess portions

$$f = f^{\text{id}} + f^{\text{ex}}. \quad (4)$$

The ideal part of the free energy density is given by a straightforward generalization of the free energy of an ideal gas as

$$\beta f^{\text{id}} = \int dR \rho(R) [\ln \rho(R) - 1], \quad (5)$$

with $\beta = 1/(k_B T)$. For the case of the rectangular distribution, the ideal free energy density is simply

$$\beta f^{\text{id}} = \rho (\ln \rho - 1) - \rho \ln(\bar{R}w). \quad (6)$$

We calculate the excess free energy density, f^{ex} , of the polydisperse fluid from the general equation of state given by Salacuse and Stell.¹⁹ This equation of state is a straightforward generalization of the highly successful EOS for an arbitrary hard-sphere mixture²⁰ first considered by Mansoori *et al.* The Mansoori EOS has been checked against simulation data by a number of authors and agreement is generally excellent. The free energy per particle ($\mathcal{F} = F/N$) is then $\mathcal{F}_f = (f_f^{\text{id}} + f_f^{\text{ex}})/\rho$.

Now we consider the free energy of the fractionated solid phase. Since as mentioned above, we expect the number of crystals to depend upon the overall polydispersity σ of the parent distribution, we consider the general case of P coexisting crystals. In order to establish some relation between the parent distribution $\rho(R)$ and the sub-distribution, $\rho_i(R)$, found in the i th crystal, we make two assumptions. First, we choose the distribution in each crystal to be rectangular and second, to keep the theory computationally manageable, we force the width (or polydispersity) to be equal in each of the P coexisting phases. With these two restrictions the housekeeping of the fractionation process is straightforward. The i th crystal, for instance, contains all N_i particles whose diameters lie between $\bar{R}[1 - w_s(1 + (P/2) - i)]$ and $\bar{R}[1 - w_s((P/2) - i)]$ with w_s , the width of the crystal distribution, given by $w_s = w/P$. The mean diameter of particles in the i th crystal is then simply given as

$$\bar{R}_i = \bar{R} \left[1 - \frac{w_s}{2} (1 + P - 2i) \right] \quad (7)$$

and the polydispersity of each crystal is $\sigma_s = \sigma/P$. The diameter distribution in the i th crystal is then

$$\rho_i(R) = \rho_i \begin{cases} 0 & R < \bar{R}_i(1 - w_s/2) \\ (\bar{R}_i w_s)^{-1} & \bar{R}_i(1 - w_s/2) \leq R \leq \bar{R}_i(1 + w_s/2), \\ 0 & R > \bar{R}_i(1 + w_s/2) \end{cases} \quad (8)$$

at an overall density of $\rho_i = N_i/V_i$ with V_i the volume of the i th phase. Although the number of particles in each crystal phase is the same for all crystals and equal to N/P (since the polydispersity of each crystal is assumed equal) the volume V_i of each phase is so far undetermined. To fix the volume, or equivalently the number density ρ_i , of each crystal we use the fact that the crystals are in equilibrium with each other.

This constraint is straightforward to apply since, in our model of the partition, no particle may exist in anymore than one crystal. Consequently we do not need to consider exchange of particles. Equilibrium simply requires that the osmotic pressure of each crystal, Π_i , be fixed and equal to an external pressure of, say, Π

$$\Pi_i(\rho_i, \sigma_s, \bar{R}_i) = \Pi. \quad (9)$$

With the density of each crystal phase determined, the total number density of the set of P coexisting crystals is then

$$\bar{\rho}_s = \frac{P}{\sum_{i=1}^P (1/\rho_i)} \quad (10)$$

and the corresponding composite packing fraction is $\bar{\phi} = (\pi/6)\bar{\rho}_s\bar{R}^3(1+w^2/4)$. The mean free energy per particle is

$$\bar{\mathcal{F}}_s^P = \frac{1}{P} \sum_i \frac{f_i}{\rho_i}, \quad (11)$$

where f_i is the free energy density of the i th crystal.

To complete our model for the fractionated phases we need an expression for the excess free energy of a polydisperse crystal. For that purpose we use a scaled particle theory. Since the details have been described elsewhere¹⁴ we just outline the approach here. The model exploits the picture of particles in a solid as being confined in cells or cages formed by the neighbors from which they cannot escape. While in a monodisperse crystal the cells are all identical, in a polydisperse crystal the size and shape of the cell varies. The idea is to recognize that one can allow for the variability in the cell shape to a first approximation, by considering just a finite number of different-sized neighbors. The number of different-sized particles is determined by the accuracy with which the properties of the finite mixture approximate those of the polydisperse system. If the excess free energy of the polydisperse system is a function of the first p moments of the diameter distribution [$p/2$] different-sized spheres are needed to match the diameter moments of the continuous distribution ($[x]$ is the smallest integer not less than x). For a polydisperse system of hard spheres, highly successful mean-field theories such as the Percus–Yevick approximation suggest that only four diameter moments are significant.¹⁹ In this case, the properties of a polydisperse system should be well approximated by a binary mixture of spheres, chosen so that the first four moments of the polydisperse and binary distributions are equal. The two diameter distributions are “equivalent” and all excess properties are, to a first approximation, equal. For the rectangular distribution the equivalent binary distribution has an equal number of large and small spheres with diameters $\bar{R}_i(1+\sigma_s)$ and $\bar{R}_i(1-\sigma_s)$, respectively. Specifically then, we equate the excess free energy of the polydisperse crystal with that of an equivalent binary substitutional crystal. For the evaluation of the latter we take advantage of the analytical expressions quoted by Kranendonk and Frenkel²¹ as fits to Monte Carlo simulation results. Combining the excess free energy with the ideal free energy density,

$$\beta f_i^{\text{id}} = \rho_i(\ln \rho_i - 1) - \rho_i \ln(\bar{R}_i w_s) \quad (12)$$

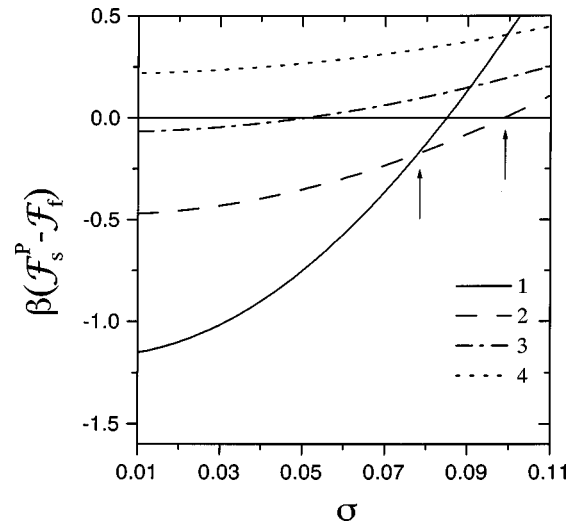


FIG. 1. The free energy difference per particle, at a constant packing fraction of $\phi=0.6$, between polydisperse crystalline and fluid phases as a function of polydispersity. The number of coexisting crystals is detailed in the legend. The arrows mark the polydispersity limits between which the fractionated binary crystals are stable.

yields the free energy density f_i of the i th crystal. Finally, we note that our model for the polydisperse crystal implicitly assumes that all different-sized spheres are placed randomly on the sites of a common fcc lattice. At high polydispersities, the smallest particles in the distribution could also be accommodated within the interstices of a crystal of larger particles. The current calculations ignore this possibility and so are valid only for polydispersities of $\sigma \lesssim 0.3$.

Putting everything together, we now calculate the difference free energy per particle, $\Delta \mathcal{F}^P = \bar{\mathcal{F}}_s^P - \mathcal{F}_f$, between the polydisperse fluid and the fractionated set of P crystals as follows. The overall particle density distribution of either the set of crystals or the polydisperse fluid is characterized by identical values for the overall volume fraction $\bar{\phi}$, the polydispersity σ and the mean diameter \bar{R} . For fixed $\phi = \bar{\phi}$, σ and \bar{R} , the free energy of the fluid \mathcal{F}_f is calculated from Eqs. (6) and the Mansoori EOS. Combining Eqs. (9) and (10) we see that the overall volume fraction $\bar{\phi}$ of the solid phases (or equivalently the mean density $\bar{\rho}_s$) may be considered as a function of the osmotic pressure Π . Inverting this relation yields the osmotic pressure Π and so, from Eq. (9), the densities ρ_i of each of the coexisting crystals which taken together have an overall volume fraction of $\bar{\phi}$. Knowing the density, polydispersity $\sigma_s = \sigma/P$ and mean diameter R_i [from Eq. (7)] of each crystal it is straightforward to calculate the corresponding free energy density f_i and the mean free energy $\bar{\mathcal{F}}_s^P$ of the multiple crystals from Eq. (11).

III. RESULTS

We now present in detail results for the stability of a system of polydisperse hard spheres obtained from the theory described above. In Fig. 1, we show the free energy difference, $\beta \Delta \mathcal{F}^P$, between the fractionated crystals and the fluid phase as a function of polydispersity, for the represen-

tative density of $\phi=0.60$. The first question to be addressed is the relative stability of the various fractionated crystals and the fluid phase.

Referring to Fig. 1, we see that for low levels of polydispersity, at this density, the crystal has a significantly lower free energy than the fluid phase. However, with increasing polydispersity, the stability of the polydisperse crystal reduces rapidly until for $\sigma \geq 0.084$ the unfractionated polydisperse crystal is unstable relative to the fluid phase. The origin of this behavior lies in the different ways polydispersity affects the maximum packing fraction, or equivalently the free volume, of ordered and disordered structures. In a fluid, smaller particles are free to pack in the cavities between larger particles and so the free volume and thus the entropy increases with polydispersity. Conversely, the periodicity of a crystal causes the free volume and entropy of a polydisperse crystal to decrease with increasing polydispersity. Consequently the free energy of a fixed-density polydisperse crystal will diverge at a critical level of polydispersity at which the fluid free energy will remain finite. Second, we note from Fig. 1 that at low polydispersities, fractionating the distribution into two or more crystals always raises the free energy of the solid state. This is because of the loss of entropy of mixing as the diameter distribution is split up. The contribution to the free energy difference, $\beta\Delta\mathcal{F}^P$, due to the loss of entropy of mixing is simply:

$$\beta\Delta\mathcal{F}_{\text{mix}}^P = \ln P \quad (13)$$

for fractionation into P crystal phases which is very close to the differences seen in Fig. 1 as $\sigma \rightarrow 0$. However, at finite polydispersities, Eq. (13), does not give a reasonable estimate of the free energy differences between the various sets of crystals. As is evident, the free energy $\beta\Delta\mathcal{F}^P$ reduces with increasing polydispersity. The reduction being smaller as the number of crystals considered increases. This is because the polydispersity of each fractionated crystal drops as the total number of crystals, between which the overall distribution is split, increases. For instance, fractionating a distribution with a polydispersity of 6% between two phases would result in crystals with 3% polydispersity, three phases would lead to 2% polydispersity and so on. As the polydispersity of each of the individual crystals decreases the influence of the divergence of the free energy at the close-packing limit is reduced and so the free energy is less affected by the overall polydispersity. As a consequence the fractionated two-crystal phase takes the place of the polydisperse single-phase crystal, as the state of lowest free energy, for $\sigma > 0.078$ and remains the most stable phase until $\sigma = 0.099$, at which point the fluid appears.

By a procedure similar to that described above, we have mapped out the range of stability of the polydisperse hard sphere system for $\sigma \leq 0.20$. Our results are shown in Fig. 2. The regions are labeled by the number of coexisting crystals which minimize the total free energy of the polydisperse system while the boundaries indicate the specific densities and polydispersities at which competing phases have equal free energies. As is evident, there are appreciable areas of density and polydispersity where fractionation into multiple crystals is predicted.

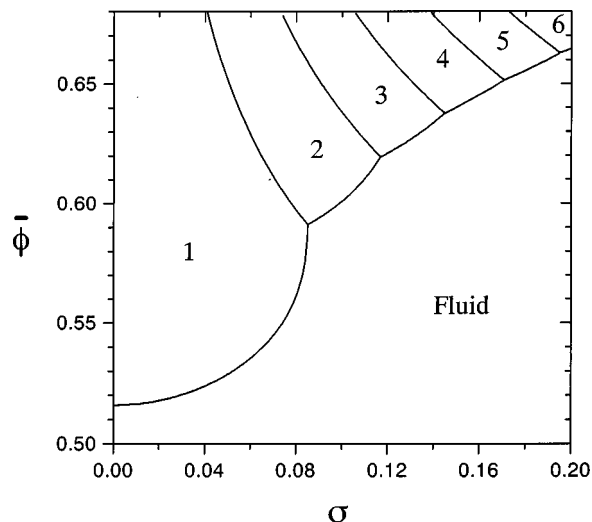


FIG. 2. The stability diagram of a polydisperse hard-sphere mixture. In each region of volume fraction ϕ and polydispersity σ the phase with the lowest free energy is indicated. Crystalline regions are labeled by the number of coexisting crystal phases.

At low volume fractions, $\phi < 0.516$, the polydisperse fluid is the most stable phase at all polydispersities. However, with an increase in packing fraction a crystalline phase takes the place of the polydisperse fluid as the most stable phase. The nature of the crystalline phase depends on the magnitude of the polydispersity σ . So while for $\sigma < 0.085$ we have crystallization into the usual single polydisperse crystal, with increasing polydispersity the fluid fractionates upon solidification into a rapidly increasing number of crystals. The diagram gets more and more complicated as the polydispersity grows since, by necessity, the number of crystalline phases required to accommodate the increasing width of the diameter distribution increase. So while for polydispersities in the range $0.085 < \sigma < 0.117$ two fractionated crystals are first formed, three crystals are required for $0.117 < \sigma < 0.145$, four for $0.145 < \sigma < 0.171$, five for $0.171 < \sigma < 0.195$ while at $\sigma = 0.20$ complete crystallization requires six different crystal phases. Furthermore, we note that as the polydispersity increases the packing fraction at which the fluid becomes unstable increases from $\phi = 0.516$ at $\sigma = 0$ to $\phi = 0.665$ at $\sigma = 0.20$. The degree of fractionation predicted varies with the overall level of polydispersity. Referring to Fig. 3, we see that the polydispersity of the crystal(s) at the fluid–solid boundary reaches a maximum of 0.085 before on average falling with increasing fluid polydispersity, although in from far a continuous fashion. Where fractionation occurs, Fig. 3 reveals that the polydispersity of each crystal formed is considerably lower than the critical polydispersity, estimated here as $\sigma_c \approx 0.085$.

In addition to the fluid–multiple crystal transitions discussed above, Fig. 2 reveals that there is a further sequence of demixing transitions in the solid phase. Compressing a polydisperse crystal causes a solid-state phase separation in which the diameter distribution is fractionated. For instance a polydisperse crystal with $\sigma = 0.08$ is stable up to a density of $\phi = 0.597$. At this point the system separates into two crystals, each of polydispersity $\sigma = 0.04$, which are stable until a

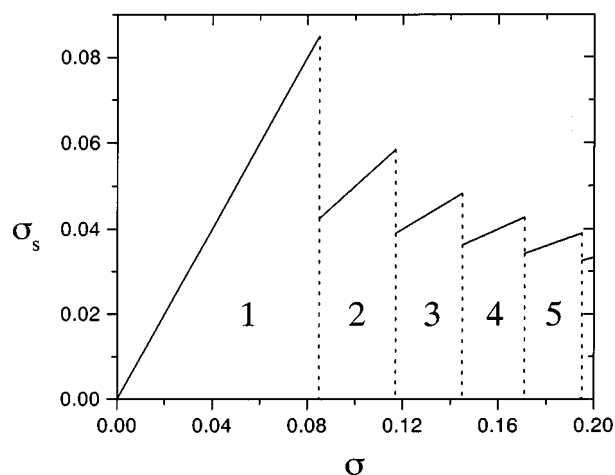


FIG. 3. The polydispersity, σ_s , of the fractionated crystalline phase formed at the fluid–solid boundary as a function of the fluid polydispersity σ .

total density of $\phi=0.667$ is reached. Further compression results in three crystals, followed at still high densities by a cascade of demixing transitions. The explanation for this behavior lies in the effect of polydispersity on the limiting packing fraction of a crystal. As mentioned previously, the density at which the free energy of a polydisperse crystal starts to diverge reduces with increasing polydispersity. As a polydisperse crystal is compressed there comes a point at which the reduction in the excess free energy which occurs when the polydispersity is reduced is sufficient to exceed the increase in the ideal free energy of mixing after fractionation. At this point the crystal phase separates.

Finally, we emphasize that we have calculated only the stability boundaries, not the full equilibrium phase diagram of a system of polydisperse spheres. The reason for this is that a full calculation of the phase equilibria, particularly in view of the large number of competing phases found in this work, would be a large and complicated problem. However, we expect our stability diagram (Fig. 2) to be a useful guide to the form of the phase diagram. Confirmation of this point of view is provided by the comparison, seen in Fig. 4, between the current model and the fluid–single crystal coexistence region established in earlier work.¹⁵ The dashed curves indicate the positions of the polydisperse cloud-point boundaries and were calculated by a novel moment projection method using, as input, polydisperse free energies similar to those described above. Referring to Fig. 4, we see that the stability boundary lies approximately midway between the two coexistence densities. Inspection of Fig. 4 reveals, rather intriguingly, that the polydisperse point of equal concentration, marked by the large circle in Fig. 4, is practically coincident with the lowest density at which the binary system of fractionated crystals is stable. This seems to be a chance occurrence. However, the proximity of the two points suggests that, at equilibrium, the re-entrant melting predicted in Ref. 15 will in fact be pre-empted by a solid-state phase separation.

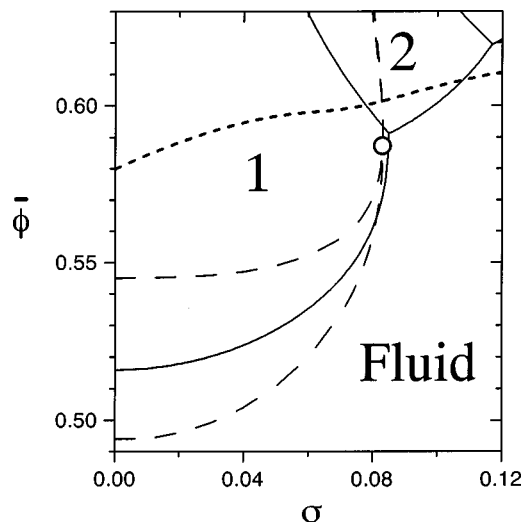


FIG. 4. A comparison between the current stability diagram (solid lines) and the fluid–solid coexistence predicted in Ref. 15 (dashed lines). The large circle marks the position of the polydisperse point of equal concentration. The thick dotted line denotes the estimated location of the polydisperse glass transition.

IV. DISCUSSION AND CONCLUSIONS

We have analyzed the stability of a polydisperse fluid of hard spheres with respect to a process of simultaneous fractionation and crystallization. Although the model is quite simple we find several interesting features. In particular, we predict that for a sufficiently polydisperse system of hard-sphere fractionation occurs upon solidification. The fluid diameter distribution separates into a number of fractions of narrower polydispersity which then crystallize. Furthermore, we find that compressing a polydisperse crystal induces a sequence of demixing transitions in the crystal.

To keep the theory presented here manageable we have been forced to make a number of assumptions. We have, for instance, imposed a somewhat arbitrary model for the fractionation process. In particular we have assumed that a rectangular diameter distribution fractionates into a number of equal-width daughter distributions, each of which is also rectangular in form. In principle, we could relax the constraint of equal width. However, since the densities of the coexisting crystals are similar it seems likely that this modification would have little effect. The more critical restriction is probably the assumption made for the form of the daughter distribution. However, in view of the relative insensitivity of polydisperse systems to the detailed form chosen for the diameter distribution, we expect that the current predictions will be in at least qualitative if not quantitative agreement with more rigorous calculations, when available.

We now speculate briefly on the feasibility of observing solid-state fractionation in experiments on hard-sphere colloids. The first point to note is that fractionation requires colloid diffusion over distances comparable to the size of the growing crystallite. The rate of such large scale diffusive motion reduces with increasing colloid density, as a result of caging effects, and essentially vanishes at the glass transition density, ϕ_g .³ For uniformly sized hard-sphere simulations²² find a long-lived metastable glassy state around $\phi_g=0.58$

which persists up to the random close-packing limit at $\phi_{\text{rcp}} = 0.64$. The glass transition in a system of polydisperse hard spheres has not been studied to the best of our knowledge although Schaertl and Sillescu²³ have estimated ϕ_{rcp} as a function of polydispersity from simulation. Assuming a simple linear relationship between the two densities gives a crude estimate of the glass transition density as $\phi_g(\sigma) \approx (0.58/0.64)\phi_{\text{rcp}}(\sigma)$. Referring to Fig. 4, we see that if this estimate for the glass transition is used, then fractionated crystallization might be experimentally observable for polydispersities in the narrow range $0.08 < \sigma < 0.11$ where diffusive motion is still possible although slow. If conversely, the dynamics of the fractionation process turn out to be appreciably slower than the experimental timeframe then experiments should follow our earlier predictions¹⁵ and exhibit a polydisperse point of equal concentration. A clear resolution of this ambiguity must await experiment.

Finally, our results suggest a possible explanation for the apparently anomalous simulations reported by Bolhuis and Kofke.¹⁰ In contrast with other theoretical work, this study found that: (i) the particle size distributions in the fluid and crystal phases were significantly different and (ii) that the coexistence region although initially narrowing with increasing polydispersity finally widened. The phase diagram was traced out by integrating along the fluid–crystal coexistence line. Implicit in this approach is the assumption that only one crystalline phase exists at the fluid–solid boundary. Referring to Fig. 2, we envisage that at the point where two polydisperse crystals become stable the simulation will follow one of the two fluid–solid branches until it halts at the discontinuity marking the start of the three-crystal region. With this picture in mind, we may readily account for the obser-

vation that at the point, where the simulation could no longer follow the fluid–solid boundary, the crystal polydispersity was almost exactly half that of the fluid value. At the same time, we note that their limiting polydispersity ($\sigma = 0.118$) lies close to our estimate for the highest polydispersity (0.117) at which two polydisperse crystals remain the equilibrium phase.

- ¹J.-P. Hansen and I. R. McDonald, *Theory of Simple Liquids* (Academic, New York, 1986).
- ²W. B. Russel, D. A. Saville, and W. R. Schowalter *Colloidal Dispersions* (Cambridge University Press, Cambridge, 1989).
- ³P. N. Pusey, in *Liquids, Freezing and Glass Transition*, edited by J. P. Hansen, D. Levesque, and J. Zinn-Justin (North Holland, Amsterdam, 1991), Chap. 10, pp. 763–942.
- ⁴P. N. Pusey and W. van Meegen, *Nature (London)* **320**, 340 (1986).
- ⁵S. E. Paulin and B. J. Ackerson, *Phys. Rev. Lett.* **64**, 2663 (1990).
- ⁶P. B. Warren, preprint (1998).
- ⁷J. A. Cuesta, preprint, cond-mat/9807030 (1998).
- ⁸R. P. Sear, preprint, cond-mat/9805201 (1998).
- ⁹E. Dickinson and R. Parker, *J. Phys. (France) Lett.* **46**, L-229 (1985).
- ¹⁰P. G. Bolhuis and D. A. Kofke, *Phys. Rev. E* **54**, 634 (1996).
- ¹¹S. E. Phan, W. B. Russel, J. Zhu, and P. M. Chaikin, *J. Chem. Phys.* **108**, 9789 (1998).
- ¹²J. L. Barrat and J. P. Hansen, *J. Phys. (France) Lett.* **47**, 1547 (1986).
- ¹³R. McRae and A. D. J. Haymet, *J. Chem. Phys.* **88**, 1114 (1988).
- ¹⁴P. Bartlett, *J. Chem. Phys.* **107**, 188 (1997).
- ¹⁵P. Bartlett, preprint (1998).
- ¹⁶L. D. Landau and E. M. Lifshitz, *Statistical Physics*, 3rd ed. (Pergamon, Oxford, 1980).
- ¹⁷P. N. Pusey, *J. Phys. (France) Lett.* **48**, 709 (1987).
- ¹⁸P. Bartlett and J. P. Voisey (unpublished).
- ¹⁹J. J. Salacuse and G. Stell, *J. Chem. Phys.* **77**, 3714 (1982).
- ²⁰G. A. Mansoori, N. F. Carnahan, K. E. Starling, and T. W. Leland, *J. Chem. Phys.* **54**, 1523 (1971).
- ²¹W. G. T. Kranendonk and D. Frenkel, *Mol. Phys.* **72**, 715 (1991).
- ²²L. V. Woodcock, *Ann. (N.Y.) Acad. Sci.* **37**, 274 (1981).
- ²³W. Schaertl and H. Sillescu, *J. Stat. Phys.* **77**, 1007 (1994).